Original Research

Angiogenic and anti-inflammatory properties of azadirachtin A improve random skin flap survival in rats

Ji-Bing He, Miao-Jie Fang, Xin-Yi Ma, Wen-Jie Li and Ding-Sheng Lin

Department of Hand Surgery, The Second Affiliated Hospital and Yuying Children's Hospital of Wenzhou Medical University, The Second Clinical College of Wenzhou Medical University, Wenzhou 325027, China.
Corresponding author: Ding-Sheng Lin. Email: lindingsheng@gmail.com

Impact statement

In plastic and reconstructive surgery, skin flap necrosis often occurs. How to improve the clinical application of skin flaps is a problem that people now look forward to solving. Drug therapy is one of the research focuses to improve skin flap survival. Our research found that Azadirachtin A promotes random skin flap survival by improving the blood supply, reducing tissue inflammation, and inhibiting flap ischemia reperfusion injury. These findings suggest that Azadirachtin A is a potential therapeutic agent for random skin flap necrosis in clinical application.

Abstract

Random skin flaps are widely used to repair tissue defects. However, the distal flap regions are prone to ischemic necrosis, limiting clinical applications. Azadirachtin A, a fruit extract from the neem, improves tissue blood supply and metabolism, reduces cell swelling, promotes tissue healing, and prevents venous thrombosis. We explored whether it enhances random skin flap survival. Fifty-four Sprague-Dawley rats were divided into control, low-dose, and high-dose Azadirachtin A-treated groups using a random number table. We used an improved version of the McFarlane technique to create flaps. On day 2, superoxide dismutase and malondialdehyde levels were measured. Tissue slices prepared on day 7 were stained with hematoxylin and eosin. The expression levels of vascular endothelial growth factor (VEGF), toll-like receptor 4 (TLR4), nuclear factor kappa-B (NF-kB), interleukin-1β (IL-1β), interleukin-6 (IL-6), and tumor necrosis factor-α (TNF-α) were immunohistochemically assayed. Microcirculatory blood flow was measured via laser Doppler blood flowmetry. Flap angiography was performed using the lead-oxide gelatin injection technique. And the azadirachtin A groups exhibited a greater mean flap survival area, an improved mean blood vessel density, a greater blood flow, and higher superoxide dismutase and VEGF levels, especially at the high dose. Azadirachtin A markedly reduced the levels of TNF-α, IL-6, IL-1β, TLR4, and NF-kB. These findings suggest that azadirachtin A promotes random skin flap survival by improving the blood supply, reducing tissue inflammation, and inhibiting flap ischemia reperfusion injury.

Keywords: Azadirachtin A, necrosis, random skin flap, inflammation, VEGF, ischemia/reperfusion injury

Experimental Biology and Medicine **2020; 245: 1672–1682. DOI: 10.1177/1535370220951896**

Introduction

As the color and texture of random skin flaps are similar to those of recipient tissues, they find many applications and are widely used by plastic surgeons to repair tissue deformities and cover skin defects caused by trauma, tumor resection, or congenital disease. However, such flaps exhibit certain clinical limitations. Given the lack of axial blood vessels, it is necessary to rely on percutaneous blood vessels emanating from the tissue pedicle to supply blood and accept the venous return[1]; good nutrition is essential for flap survival. Therefore, the aspect ratio of a random flap is constrained. When the length:width ratio exceeds 1.5–2:1, the distal part of the flap may exhibit necrosis caused by dystrophic metabolism after transfer.[2] Flap survival is affected by blood circulation, metabolic factors, and the extent to which tissue tolerates ischemia and hypoxia.[3] After random flap placement, a new vascular ganglion begins to form, running from the pedicle flap bed in a distal direction; angiogenesis is reduced at the distal end. After flap placement, vascular regeneration/reperfusion and recovery of the blood supply trigger ischemia/reperfusion injury (IRI) and necrosis.[4] IRI features both oxidative stress and apoptosis; these in turn trigger flap necrosis. Therefore, promotion of angiogenesis, improvement of local blood circulation, inhibition of inflammatory mediator production, alleviation of IRI, and reductions in

oxidative stress and cell apoptosis when the skin flap length:width ratio is increased are key in terms of improving the success rate of random flap placement[5]; this is of major clinical concern.

Natural compounds often exhibit a wide range of pharmacological activities and are used in traditional medicine as alternatives to drugs for the treatment of various diseases.[6] In recent years, neem has received a good deal of attention, being widely used to treat diseases. Azadirachtin A (AzaA; Figure 1; an Indian folk medicine) is a water extract of neem (*Azadirachta indica A. Juss*) leaves, flowers, seeds, fruits, roots, and bark that improves tissue blood supply and metabolism, reduces cell swelling, promotes tissue healing, counters apoptosis, inhibits oxidative stress, and prevents venous thrombosis.[7,8] AzaA also exhibits anti-inflammatory and immunomodulatory activities,[9,10] thus enhancing the survival of random skin flaps in rats. The efficacy of Aza A extracts may be attributable to the contained sugars.[11,12]High-performance liquid chromatography (HPLC) analyses have revealed that AzaA contains major bioactive compounds including phytosterols, triterpenoids, and flavonoids.[8] Phytosterols generally exhibit antioxidant, anti-inflammatory, and antibacterial activities; triterpenoids stimulate the immune system; and flavonoids exhibit antioxidant and anti-inflammatory properties and reduce lipid levels, not only slowing cell necrosis but also improving blood vessel distribution and promoting wound-healing.[10] The wound-healing effects of AzaA may be attributable to these active components.

Given the traditional applications and reported pharmacological activities of AzaA, the roles played by vascular endothelial growth factor and cytokines in terms of flap survival, and the presence of compounds with known antioxidant and anti-inflammatory properties, we hypothesized that AzaA might improve the survival rate of transplanted random skin flaps. Here, we established a rat model of very wide, random flap placement to verify our hypothesis.

Materials and methods

Reagents

AzaA (HPLC-UV purity $\geq$ 95%) was purchased from Wuhan Yuancheng Co-creation Technology Co. Ltd. (Wuhan, China). Tumor Necrosis Factor-α (TNF-α) ELISA kits (XLPCC, China, Cat: xl-Er0359), Interleukin-6 (IL-6) ELISA kits (XLPCC, China, Cat: xl-Er0196) were purchased from Xinle Biological (Shanghai, China). Antibodies to vascular endothelial growth factor (VEGF) (Affinity Biosciences, USA, Cat: AF5131), Nuclear factor-kB (NF-kB) (Affinity Biosciences, USA, Cat: AF5006), TNF-α (Affinity Biosciences, USA, Cat: AF7014), IL-6 (Affinity Biosciences, USA, Cat: DF6087), Interleukin-1B (IL-1β) (Affinity Biosciences, USA, Cat: AF5103), and toll-like receptor 4 (TLR4) (Affinity Biosciences, USA, Cat: AF7017) were purchased from Affinity Biosciences (Ohio, USA). Malondialdehyde (MDA) and superoxide dismutase (SOD) assay kits were purchased from Nanjing Jiancheng Bioengineering Institute (Nanjing, China).

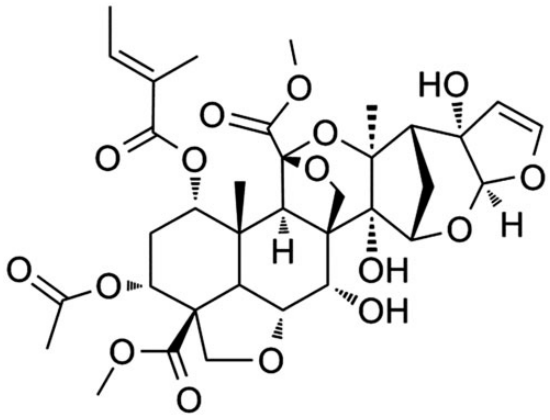

Figure 1. The chemical structure of Azadirachtin A.

Animals

Fifty-four healthy male Sprague-Dawley rats were provided by the Wenzhou Medical University Laboratory Animal Center (body mass 200–250 g, age two to three months). All the experiments involving with animals were approved by the Laboratory Animal Ethics Committee of Wenzhou Medical University (No.wydw2017-0509). The rats were divided into control, low-dose AzaA, and high-dose AzaA groups using a random number table (18 animals/group). All rats were housed in separate cages at a constant temperature of 25°C and a relative humidity of 40–60% under a standard day-night light cycle with free access to food and water. The rats were not fed on the night before the experiment. Preoperatively, anesthesia was induced by administration of 2% (w/w) pentobarbital sodium to 40 mg/kg in physiological saline, and a shaver and depilatory cream were used to completely remove the hair on the back trunk. The improved McFarlane technique (Figure 2(a)) was used to design and produce a random rectangular flap of length 9 cm and width 3 cm using the line between the two iliac ridges as the band and the dorsal ridge as the midline. To allow of convenient postoperative observation, the flap was divided into proximal (Zone I), intermediate (Zone II), and distal (Zone III) areas by reference to the blood supply (Figure 2(a)). The skin was incised and the subcutaneous tissue was separated to the shallow layer of the deep fascia. If necessary, electrocoagulation or ligation was performed when bleeding developed, and the subdermal capillary network was preserved. After blunt dissection, both symmetrical iliac arteries were cut at the flap base. After complete hemostasis was established, 4–0 medical mousse-nylon sutures were placed. All surgeries were performed by the same operator.

Azadirachtin, at 100 and 200 mg/kg/day, has been shown in previous studies to significantly reduce inflammatory damage and oxidative stress.[13] According to the pilot experiment result, we choose these therapeutic doses. After surgery, 10 g AzaA powder was ground in 1000 mL of normal saline to make a 10 mg/mL solution, rats in the low-dose and high-dose experimental groups received AzaA orally at 100 and 200 mg/kg/day respectively, while rats in the control group received the same

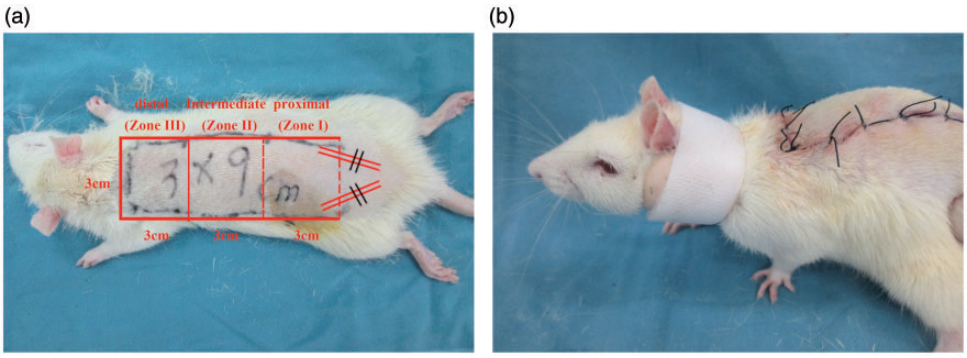

Figure 2. A random flap placed on a rat back (a) and the neck fixation ring (b). (A color version of this figure is available in the online journal.)

amount of normal saline. All rats underwent continuous gavage for seven days, and all were raised in single cages. To obviate poor flap survival caused by self-injury, all rats were fitted with neck fixation rings (Figure 2(b)).

Macroscopic assessment of flap survival areas

Macroscopic flap changes (color, tissue elasticity, texture) were recorded on day 7 after surgery. Surviving flap areas were soft pink in color with new hair growth; the necrotic areas were scabbed, hardened, and darkened, without hair growth. We took digital photographs with scale marks, imported the images to a computer, and evaluated average flap survival using Image-Pro Plus ver. 6.0 software (National Institutes of Health, Bethesda, MD, USA). The flap survival area ratio was the surviving flap surface area/total surface area $\times$ 100%.

SOD and MDA levels

Two days postoperatively, 0.5 $\times$ 0.5 cm tissue samples were excised from the middle flap areas (Zone II), the muscle layers were removed, and the samples were ground. After 1:10 dilution in ice water, the samples were homogenized at 2500 r/min, centrifuged for 10 min, and the supernatant superoxide dismutase (SOD) and malondialdehyde (MDA) levels were measured using a colorimetric and a thiobarbituric acid method, respectively.

Flap blood flow

To assess microcirculatory blood flow, six rats of each group were anesthetized and scanned using a laser Doppler flowmeter (LDF) on day 7 after surgery. MoorLDI Review ver. 6.1 software was used to measure blood perfusion in perfusion units (PUs; relative measures of microcirculatory blood flow rates in local tissue, indirectly reflecting new, flap, blood vessel status).

TNF-α and IL-6 levels

Blood samples were centrifuged at 5000$\times g$ for 15 min. The supernatants were collected and serum levels of TNF-α and IL-6 were measured via ELISA at an absorbance of 450 nm.

Gelatin-lead oxide angiography

On day 7 after operation, six rats of each group were anesthetized and normal saline at 37°C was instilled into the carotid arteries of one side to wash out all blood vessels. The body temperature was controlled to prevent vasospasm. Blood was drained via the ipsilateral jugular vein. After the liquid flowing out of the jugular vein became clear, colored, gelatin-lead oxide perfusate fluid (100 mL/kg) was slowly injected into the carotid artery using a syringe. Perfusion ceased when the fluid attained the extremities, ears, and corneas (as judged by the characteristic fluid color). The carotid artery was ligated with silk thread and the samples were refrigerated at 4°C for 12 h to facilitate gelatin aggregation. Finally, the rat dorsal flap and surrounding skin were dissected and X-ray angiography performed.

Histopathological examination

On day 7 after operation, all rats were anesthetized and killed with 100 g/L chloral hydrate (8 mL/kg). Tissue samples from Zone I, Zone II, Zone III were fixed in 10% (v/v) paraformaldehyde for 24 h, embedded in paraffin, sectioned (thickness 4 μm), and subjected to hematoxylin-and-eosin staining. Using an optical microscope, granulation formation, structural capillary changes, tissue edema, necrosis, and inflammatory infiltration were scored. The neutrophil density and the number of microvessels per unit area (mm^2) in Zone II were calculated.

Immunohistochemistry

The remaining paraffin sections were immunohistochemically processed using the streptavidin-peroxidase method to assess the expression levels of VEGF, TLR4, NF-kB, IL-1β, IL-6 and TNF-α in flap tissue. Images were obtained using the DP2-TWAIN (Olympus, Tokyo, Japan) platform operating at 400$\times$ magnification. The integrated absorbances of VEGF, TLR4, NF-kB, IL-1β, IL-6, and TNF-α were used to determine the expression levels.

Statistical analyses

All statistical analyses were performed using SPSS ver. 19 software (SPSS, Chicago, IL, USA). Data are expressed as means$\pm$standard deviations (SDs). Means of each group

were compared using Student's *t*-test. A *P*-value < 0.05 was considered to reflect statistical significance.

Results

Macroscopic evaluation of surviving areas

On postoperative day 7, Zones II and III were necrotic with dark black lesions; no necrosis was apparent in Zone I. The extent of skin flap necrosis was notably greater in the control group than in the experimental group. The control flaps were darker and exhibited larger necrotic areas (Figure 3(a)). The average survival percentage of flaps in the control, low-dose, and high-dose groups was $50.16 \pm 2.32\%$, $71.19\% \pm 2.50\%$, and $90.83 \pm 2.26\%$, respectively. The difference was significant ($P < 0.01$; Figure 3(b)).

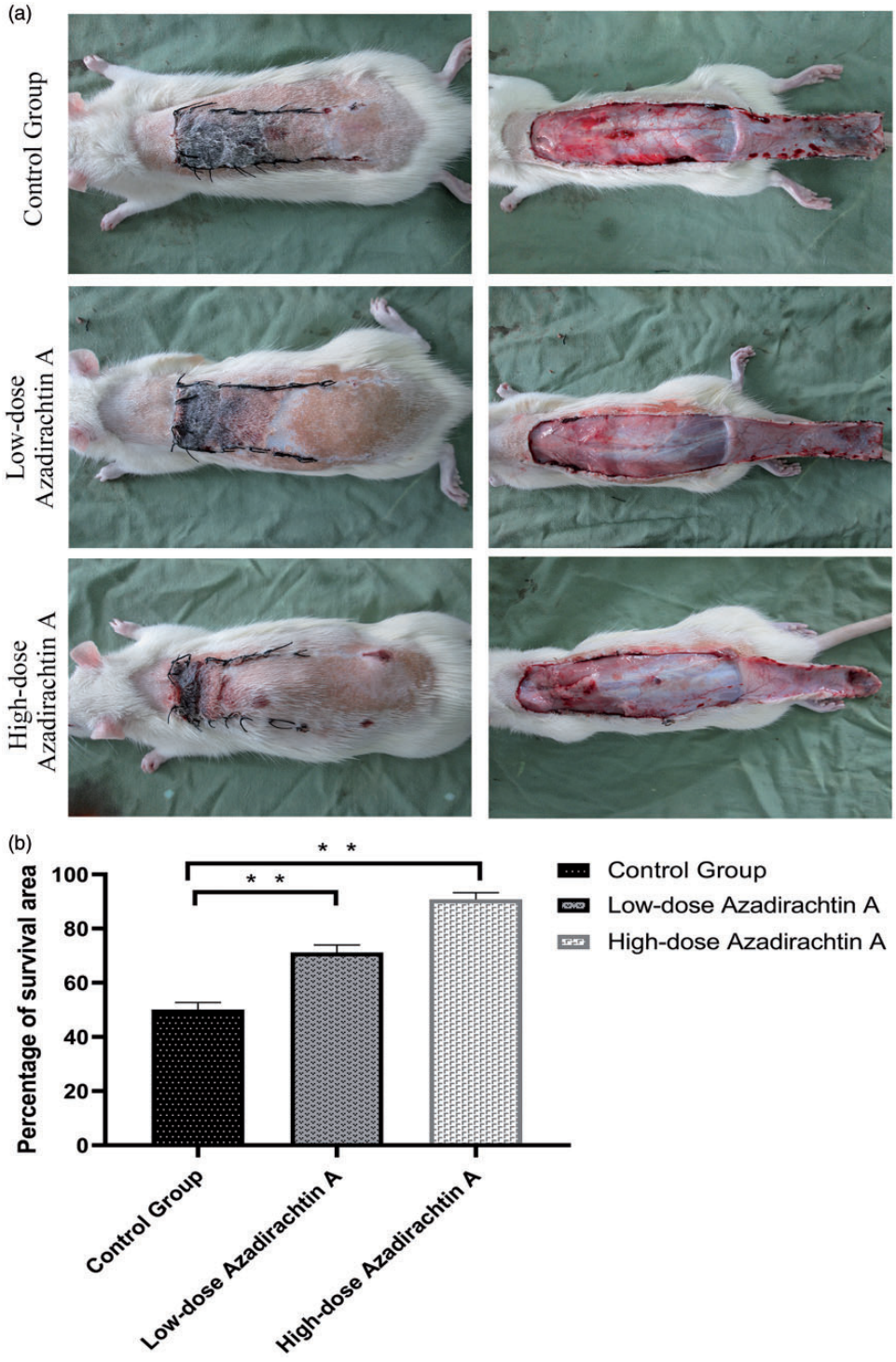

Figure 3. AzaA increased the flap survival. Digital photographs reflecting flap survival (a). Survival area percentages (b). $^{**}P < 0.01$, low-dose and high-dose AzaA groups vs. control group; $n = 6$ per group. (A color version of this figure is available in the online journal.)

Superoxide dismutase and malondialdehyde levels

The average SOD content of the high-dose AzaA group was 62.84 ± 2.99 units/mg protein, and the average SOD content of the low-dose AzaA group was 52.41 ± 2.75 units/mg protein, higher than that of the control group (23.89 ± 1.96 units/mg protein) ($P < 0.01$). The average MDA level of the high-dose AzaA group was 21.36 ± 3.00 nmol/mg protein, and the average MDA level of the low-dose AzaA group was 44.25 ± 3.60 nmol/mg protein, lower than that of the control group (70.16 ± 5.21 nmol/mg protein) ($P < 0.01$) (Figure 4(a) and (b)).

Flap blood flow

LDF images are shown in Figure 5(a). Zone II perfusion of the high-dose AzaA group (300.32 ± 45.25 PU) and low-dose AzaA group (263.15 ± 55.29 PU) was higher than that of the control group (50.73 ± 12.70 PU) ($P < 0.01$; Figure 5(b)).

TNF-α and IL-6 levels

AzaA suppressed TNF-α production compared to that of the control group (high-dose AzaA 79.06 ± 8.75 pg/mL; low-dose AzaA 116.31 ± 15.41 pg/mL; control 198.24 ± 13.55 pg/mL; $P < 0.01$; Figure 6(a)). The IL-6 data were similar (high-dose AzaA, 28.57 ± 2.41 pg/mL; low-dose AzaA, 46.82 ± 3.58 pg/mL; control, 87.84 ± 8.36 pg/mL; $P < 0.01$; Figure 6(b))

Gelatin-lead oxide angiography

Angiography clearly showed more and better-quality regenerated blood vessels in the experimental group than in the control group, particularly in the high-dose group. The extents of vascular reconstruction at the recipient site and flap edges were good. AzaA markedly increased the tissue blood supply (Figure 7).

Histopathological data

Seven days after surgery, the distal areas (Zone III) were morphologically similar in histological terms. All flaps exhibited similar changes in appearance; inflammatory cell infiltration was prominent, as were structural damage and edema. The tissue images revealed degeneration and necrosis of muscle fibers. In the proximal areas (Zone I), the AzaA group exhibited edema and inflammatory cell infiltration to a lesser extent than controls. In flap Zone II, high-dose and low-dose AzaA groups exhibited significant subcutaneous fibroblast proliferation. The granulation tissue was thin with slight tissue edema; diffuse subcutaneous hemorrhage was apparent. Control flaps were thicker than AzaA flaps and exhibited less fibroblast proliferation and neovascularization, more edema, and more inflammatory cell infiltration. (Figure 8). The neutrophil density (high-dose $22.03 \pm 4.33/mm^2$; low-dose $37.46 \pm 3.09/mm^2$) in the AzaA Zone II region was lower than in the control group ($66.14 \pm 4.44/mm^2$) (Figure 9(a)). The microvessel density (high-dose $35.98 \pm 3.99/mm^2$; low-dose $23.16 \pm 2.98/mm^2$) in the AzaA Zone II region was higher than in the control group ($12.46 \pm 2.88/mm^2$). Both differences were significant ($P < 0.01$; Figure 9(b)).

Immunohistochemical data

Immunohistochemical analyses indicated that the levels of VEGF in the control group, low-dose group, and high dose group were 1522.00 ± 312.56 IA, 2956.67 ± 351.41 IA, and 4450.50 ± 288.81 IA, respectively. The TLR4 levels of each group were 5142.17 ± 458.47 IA, 3118.00 ± 215.51 IA, and 1117.00 ± 157.09 IA, respectively. The NF-kB levels of each group were 5222.17 ± 438.09 IA, 2570.33 ± 246.92 IA, and 850.50 ± 98.08 IA, respectively. The IL-1β levels of each group are 2667.33 ± 349.93 IA, 1397.67 ± 244.81 IA, and 622.83 ± 97.02 IA, respectively. The IL-6 levels of each group were 3637.83 ± 244.24 IA, 2052.50 ± 132.85 IA, and 736.50 ± 71.94 IA, respectively. The TNF-α levels of each group levels were 3118.33 ± 249.91 IA, 1426.00 ± 212.30 IA, and 813.00 ± 125.53 IA, respectively. These observations indicate that AzaA dose-dependently regulates VEGF expression and down-regulates the expression of proinflammatory cytokines (NF-kB, IL-6, IL-1β, TLR4, and TNF-α). All between-group differences were significant ($P < 0.01$; Figure 10).

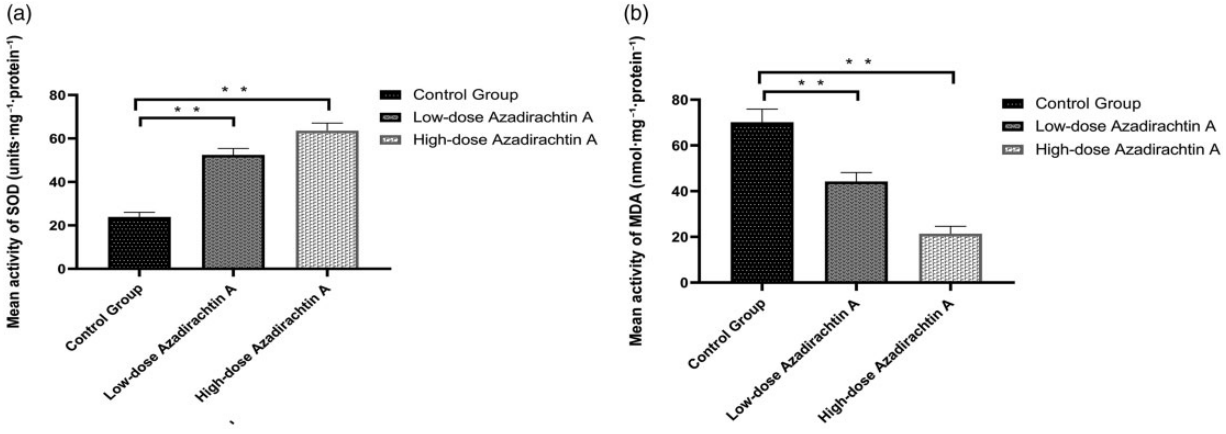

Figure 4. AzaA promoted SOD activity and downregulated MDA level. Mean superoxide dismutase activities of the control and treatment groups (a). Mean malondialdehyde levels of the control and treatment groups (b). $^{**}P < 0.01$, low-dose and high-dose AzaA groups vs. control group; $n = 6$ per group.

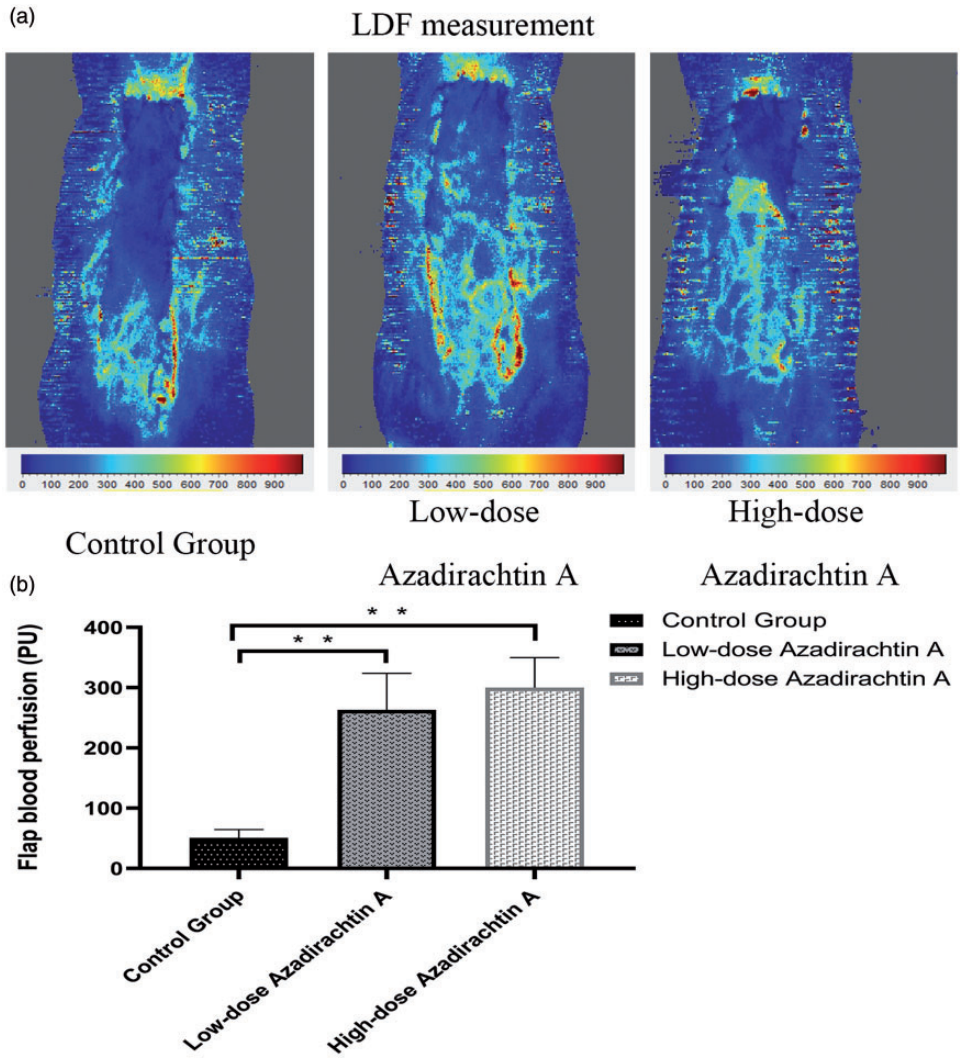

Figure 5. AzaA increased blood flow. Laser Doppler flowmetry (LDF) angiography of flaps of the control and treatment groups (a). Mean blood perfusion levels of the Zones II of each group (b). $^{**}P < 0.01$, low-dose and high-dose AzaA groups vs. control group; $n = 6$ per group. (A color version of this figure is available in the online journal.)

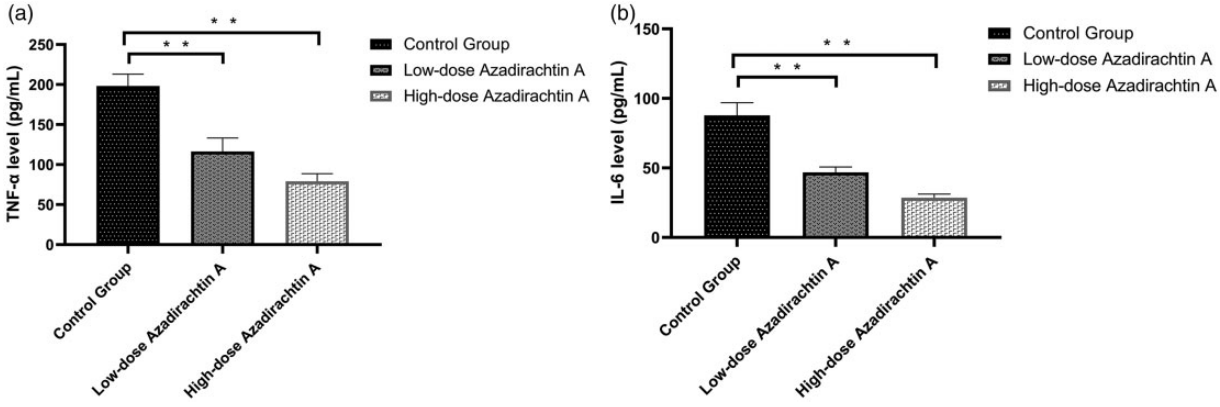

Figure 6. AzaA inhibited the expression of TNF-α and IL-6. The expression levels of TNF-α (a) and IL-6 (b) as measured via ELISA. $^{**}P < 0.01$, low-dose and high-dose AzaA groups vs. control group; $n = 6$ per group.

Discussion

Unlike the vascular systems of axial flaps, random flaps rely on existing vessels in surrounding tissues, and thus are free of the limitations of traditional flaps, including the need to carefully consider positioning and the axial vascular distribution. However, if the length:width ratio

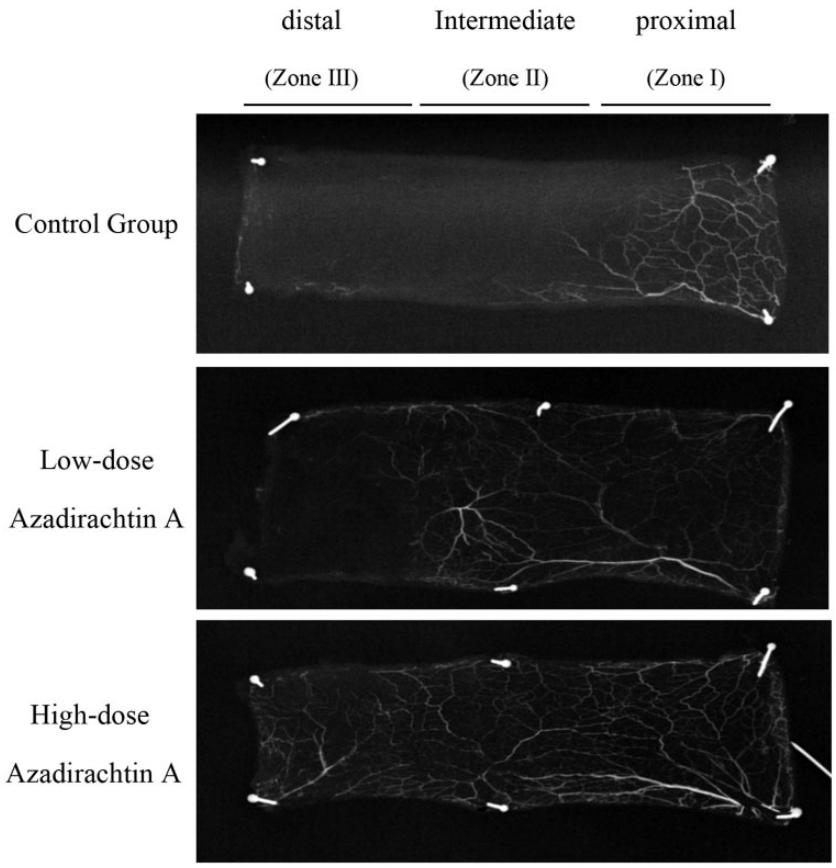

Figure 7. AzaA improved flap angiography. Lead oxide/gelatin angiographic imaging data.

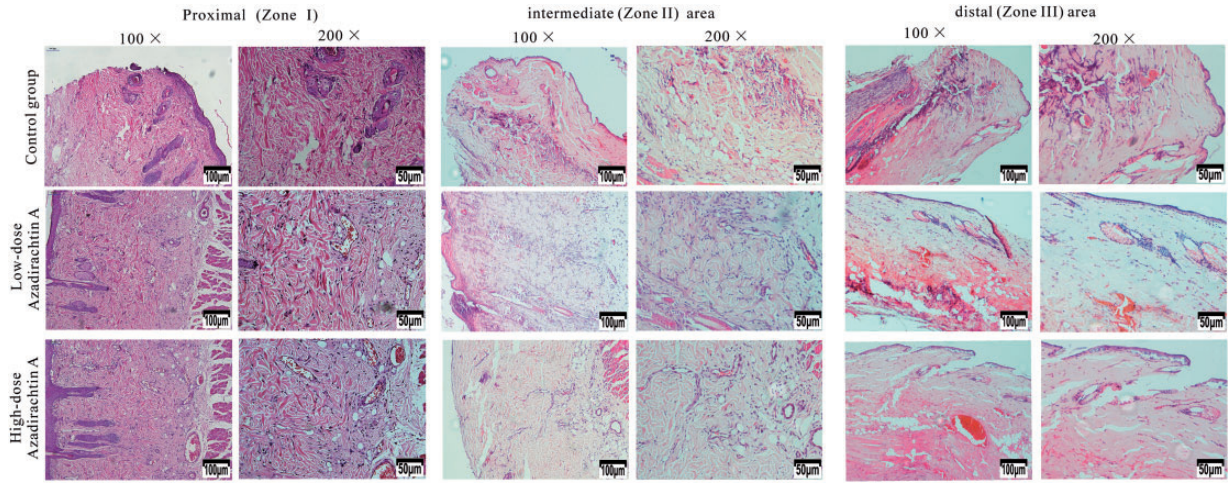

Figure 8. AzaA reduced histopathological damage. Histopathological data in Zones I, Zones II, and Zone III of flaps of the control and treatment groups. Hematoxylin and eosin staining. Magnifications: 100× and 200×. (A color version of this figure is available in the online journal.)

of a random flap exceeds a certain value, the distal part of the flap may experience nutritional/metabolic disorders triggering necrosis. Flap survival is critically dependent on flap blood perfusion pressure; the blood flow to random flaps is supplied by the pedicle. Therefore, super-long random flaps will survive only if the broken ends of blood vessels rapidly "kiss" at the wound edge; nascent capillaries then grow within the flap. We found that AzaA stimulated angiogenesis by upregulating VEGF production, reducing oxidative stress, alleviating tissue inflammation, and inhibiting IRI.

In the early stage, we found that drugs such as Naringin[14] and batroxobin[15] can promote flap survival, but AzaA shows better anti-inflammatory effects by regulating the TLR4/NF-kB pathway, reducing the release of inflammatory cytokines, and inhibiting the chemotaxis and adhesion of neutrophils.

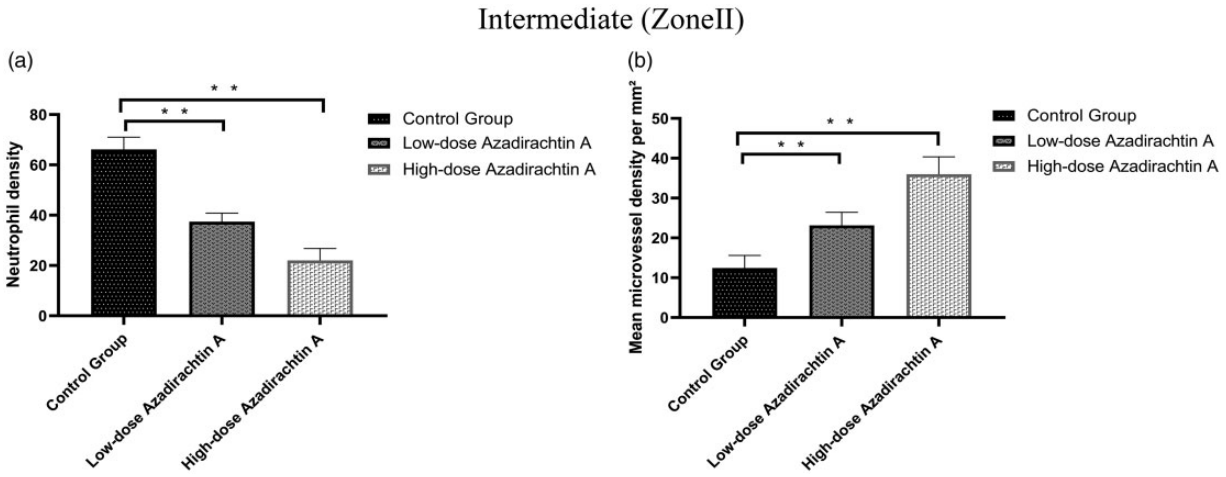

Figure 9. AzaA reduced neutrophil density and increased microvessel density. Neutrophil densities in Zones II (a). Mean microvessel densities in Zones II (b). $^{**}P < 0.01$, low-dose and high-dose AzaA groups vs. control group; $n = 6$ per group.

Inflammatory reactions develop rapidly during wound-healing. The epidermis of necrotic areas at the distal end of a random flap exhibit obvious inflammatory cell infiltration and coagulative necrosis. The greater the extent of necrosis, the more severe the inflammatory reaction. Reduction of inflammation promotes flap survival. AzaA markedly reduced TNF-α and IL-1β levels, inhibiting tissue infiltration by neutrophils and other inflammatory cells, and relieving inflammatory pain.[16] AzaA interacts with tumor necrosis factor receptors (TNFRs), inhibits TNF signaling via downstream activation of IKK, breaks down IkB-α, and inhibits activation of nuclear factor-kB (NF-kB), thereby effectively controlling inflammation.[17,18] The NF-kB pathway controls the expression of various pro-inflammatory mediators and thus plays a very important role in the inflammatory response. The NF-kB transcription factor regulates the production of cytotoxic substances such as nitric oxide, indirectly controlling apoptosis, and thus skin flap survival.[19] We found that AzaA downregulated TLR4. Toll-like receptors (TLRs) are surface transmembrane receptors that trigger both innate and adaptive immunity.[20] The receptors play key roles in inflammation and immune cell regulation, survival, and proliferation. TLR4 is involved in TLR4/NF-kB signaling, which in turn controls the immune and inflammatory responses by regulating the expression levels of immune-related factors and inflammatory transmitters. Notably, drugs exhibiting exclusively anti-inflammatory properties usually do not inhibit the nociceptive response. However, AzaA, which exhibits anti-inflammatory activity in an animal model, also suppresses pain by inhibiting inflammatory mediators and enhancing central pain management. At least in nociceptive models of pain, the activity of AzaA depends to a large extent on activation of endogenous opioid mechanisms, which control many drug antinociceptive activities.[21,22] AzaA plays useful roles in experimental models of inflammatory and noxious pain, and in models of chronic and acute inflammation.[23] Such activities are of major importance in terms of promoting skin flap survival.

We found that AzaA enhanced VEGF production. Previous studies have shown that the flap VEGF level profoundly affects flap blood vessel formation.[24,25] During early angiogenesis, VEGF regulates the proliferation, differentiation, and migration of vascular endothelial cells, promotes vasodilation and extracellular matrix formation; induces endothelial cell mitosis, promotes the formation and maturation of new blood vessel lumina, and increases the number of capillaries. VEGF reduces skin flap necrosis, enhances the anti-infective flap capacity, promotes wound-healing, and increases the survival rate of full-thickness flaps. Hematoxylin-and-eosin and immunohistochemical staining and gelatin lead oxide angiography showed that AzaA stimulated new blood vessel formation and increased the number of microvessels in ischemic skin flaps, thus enhancing both the quantity and quality of regenerated blood vessels. An improved blood supply alleviates the inflammatory response and increases the survival rate of random skin flaps.[26]

IRI is involved in the pathophysiology of random flap ischemic necrosis. IRI and inflammation engage in mutually reinforcing cascading reactions during distal necrosis development in ischemic, super-long, random skin flaps. IRI is important in terms of the inflammatory response that in turn triggers skin flap necrosis. Ischemic flap tissue generates high levels of reactive oxygen species (oxygen ions, free radicals, and peroxides) that activate both mitochondria and other downstream targets (endogenous endonucleases and protein kinases), in turn triggering programmed cell death and distal flap necrosis.[27] The levels of certain metabolites (including arachidonic acid) increase during reperfusion, in turn attracting many neutrophils to the tissue; these cells adhere to the vascular endothelium and aggravate the inflammatory response. Simultaneously, oxygen free-radical generation increases, damaging ischemic tissue cells, and activating cell–cell adhesion and neutrophil chemotaxis.[28] This further enhances neutrophil infiltration, aggravating flap tissue damage via a vicious cycle. SOD, glutathione, and catalase are well-known antioxidants that scavenge free radicals. SOD

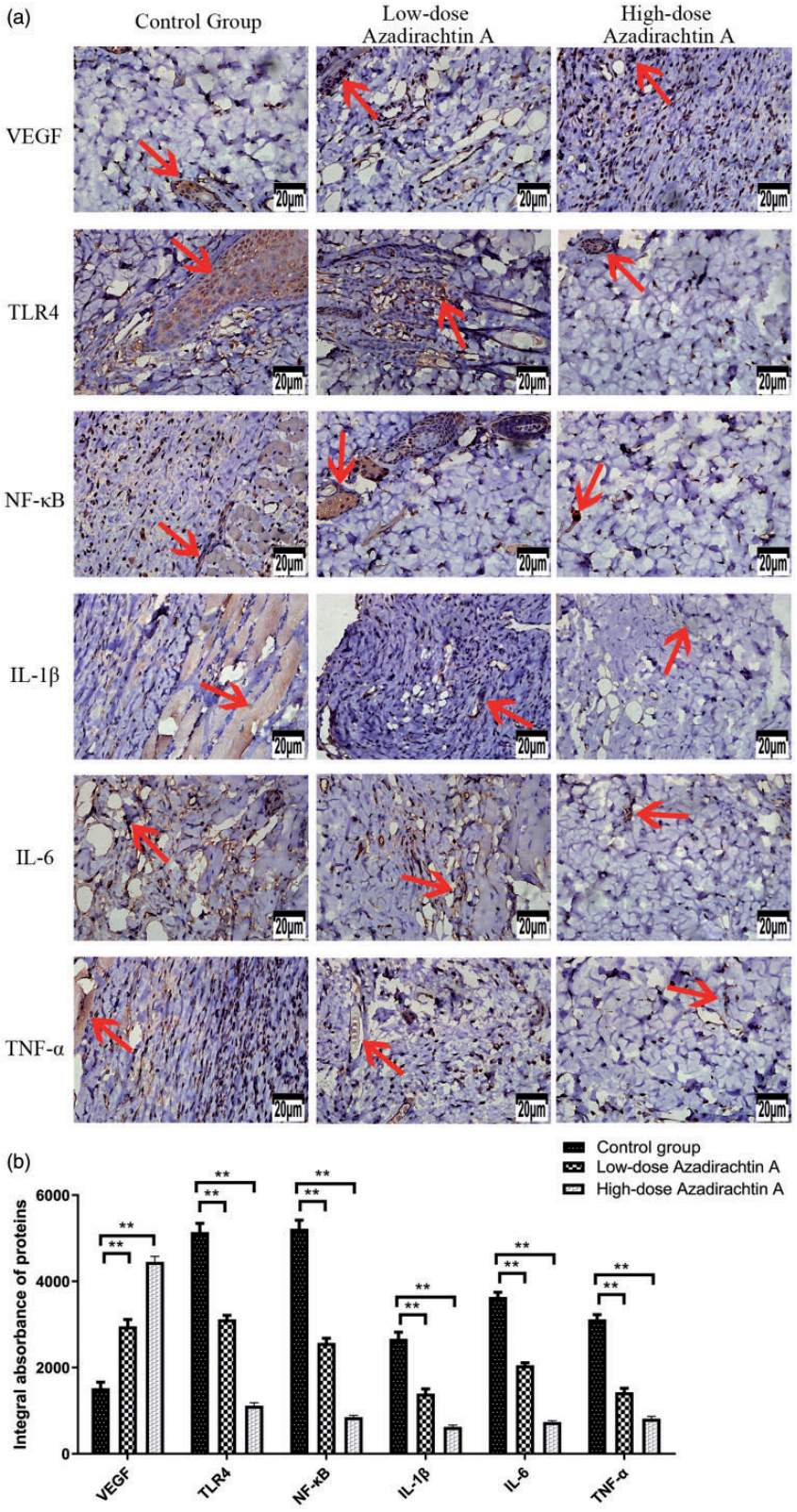

Figure 10. AzaA promoted the expression of VEGF and inhibited the expression of TLR4, NF-kB, IL-1β, IL-6, and TNF-α. The immunohistochemically derived, flap expression levels of VEGF, TLR4, NF-kB, IL-1β, IL-6, and TNF-α as revealed by the DP2-TWAIN system (Olympus, Tokyo, Japan) operating at 400$\times$ magnification (a). The integral absorbances of flap VEGF, TLR4, NF-kB, IL-1β, IL-6, and TNF-α levels in the control and treatment groups (b). $^{**}P < 0.01$, low-dose and high-dose AzaA groups vs. control group; $n = 6$ per group. Arrows indicate positive reaction. (A color version of this figure is available in the online journal.)

converts superoxide radicals into hydrogen peroxide,[29] which is then cleared by glutathione or peroxidase to protect cells[30]; this is the first-line defense of cells exposed to reactive oxygen. AzaA increased the levels of SOD, glutathione, and catalase, thus inhibiting oxidative stress. The MDA level is an important marker of tissue damage; oxidant or inflammatory stimulation upregulate tissue MDA levels. The SOD and MDA levels were measured on day 2 after operation. Immunohistochemically, AzaA increased SOD activity and decreased the MDA content, suggesting that AzaA alleviated IRI by inhibiting oxidative stress.

Although AzaA is a component of pesticides, the material is nontoxic to humans,[31] including those with diabetes, malaria, eczema, and scabies.[32] Male and female rats given oral AzaA at doses of 500, 1000, and 1500 mg/kg/day for 90 days did not exhibit any acute toxicity (salivation, coma, or death).[33] Thus, no absolute contra-indication to AzaA use was apparent. AzaA dose-dependently increased flap blood supply, relieved both IRI and pain, improved flap survival and quality, and inhibited the inflammatory response, oxidative stress, and apoptosis. Thus, it exhibits high-level economic and practical potential. However, we studied rats only. The utility of AzaA in terms of human skin graft recovery and reconstruction requires further testing.

Authors' contributions: All authors participated in the design, interpretation of the studies and analysis of the data and review of the manuscript; JBH and DSL designed the research and wrote the manuscript. JBH, XYM, MJF and WJL implemented the experiments and performed the data analysis. MJF and DSL reviewed and edited the manuscript.

DECLARATION OF CONFLICTING INTERESTS

The author(s) declared no potential conflicts of interest with respect to the research, authorship, and/or publication of this article.

FUNDING

This work was supported by the 2019 National Undergraduate Innovation and Entrepreneurship Training Program [grant number 201910343015].

ORCID iD

Ji-Bing He https://orcid.org/0000-0002-5293-2630

REFERENCES

1. Hashimoto I, Abe Y, Ishida S, Kashiwagi K, Mineda K, Yamashita Y, Yamato R, Toda A, Fukunaga Y, Yoshimoto S, Tsuda T, Nagasaka S, Keyama T. Development of skin flaps for reconstructive surgery: random pattern flap to perforator flap. *J Med Invest* 2016;**63**:159–62
2. Deng C, Wu B, Wei Z, Zhang Z, Zhang T, Wang D. A systematic study of vascular distribution characteristics and axis design of various flap types. *Med Sci Monit* 2019;**25**:721–9
3. Bobek V, Sramek D, Rokyta R, Tvrdek M. Local pharmacological preconditioning increases the survival of experimental skin flaps in rats. *Life Sci* 2005;**77**:2663–8
4. Lin R, Chen H, Callow D, Li S, Wang L, Li S, Chen L, Ding J, Gao W, Xu H, Kong J, Zhou K. Multifaceted effects of astragaloside IV on promotion of random pattern skin flap survival in rats. *Am J Transl Res* 2017;**9**:4161–72
5. Tsai TC, Tung YT, Kuo YH, Liao JW, Tsai HC, Chong KY, Chen HL, Chen CM. Anti-inflammatory effects of antrodia camphorata, a herbal medicine, in a mouse skin ischemia model. *J Ethnopharmacol* 2015;**159**:113–21
6. Calixto JB, Campos MM, Otuki MF, Santos AR. Anti-inflammatory compounds of plant origin. Part II. modulation of pro-inflammatory cytokines, chemokines and adhesion molecules. *Planta Med* 2004;**70**:93–103
7. Gautam MK, Gangwar M, Singh SK, Goel RK. Effects of azardirachta indica on vascular endothelial growth factor and cytokines in diabetic deep wound. *Planta Med* 2015;**81**:713–21
8. Fernandes SR, Barreiros L, Oliveira RF, Cruz A, Prudencio C, Oliveira AI, Pinho C, Santos N, Morgado J. Chemistry, bioactivities, extraction and analysis of azadirachtin: state-of-the-art. *Fitoterapia* 2019;**134**:141–50
9. Chattopadhyay I, Nandi B, Chatterjee R, Biswas K, Bandyopadhyay U, Banerjee RK. Mechanism of antiulcer effect of neem (azadirachta indica) leaf extract: effect on H+–K+–ATPase, oxidative damage and apoptosis. *Inammopharmacology* 2004;**12**:153–76
10. Gautam MK, Goel S, Ghatule RR, Singh A, Joshi VK. Goel Rk Azadirachta indica attenuates colonic mucosal damage in experimental colitis induced by trinitrobenzene sulfonic acid. *Indian J Pharm Sci* 2013;**75**:602–6
11. Dorababu M, Prabha T, Priyambada S, Agrawal VK, Aryya NC, Goel RK. Effect of bacopa monniera and azadirachta indica on gastric ulceration and healing in experimental NIDDM rats. *Indian J Exp Biol* 2004;**42**:389–97
12. Dorababu M, Joshi MC, Bhawani G, Kumar MM, Chaturvedi A, Goel RK. Effect of aqueous extract of neem (azadirachta indica) leaves on offensive and diffensive gastric mucosal factors in rats. *Indian J Physiol Pharmacol* 2006;**50**:241–9
13. Oyagbemi AA, Omobowale TO, Ola-Davies OE, Adejumobi OA, Asenuga ER, Adeniji FK, Adedapo AA, Yakubu MA. Protective effect of azadirachta indica and vitamin E against arsenic acid-induced genotoxicity and apoptosis in rats. *J Dietary Suppl* 2018;**15**:251–68
14. Cheng L, Chen T, Tu Q, Li H, Feng Z, Li Z, Lin D. Naringin improves random skin flap survival in rats. *Oncotarget* 2017;**8**:94142–50
15. Fang MJ, Qi CY, Chen XY, Hu PY, Wang JW, Xu PF, Jin YZ, Lin DS. Effects of batroxobin treatment on the survival of random skin flaps in rats. *Int Immunopharmacol* 2019;**72**:235–42
16. Rocha AC, Fernandes ES, Quintao NL, Campos MM, Calixto JB. Relevance of tumour necrosis factor-alpha for the inflammatory and nociceptive responses evoked by carrageenan in the mouse paw. *Br J Pharmacol* 2006;**148**:688–95
17. Schumacher M, Cerella C, Reuter S, Dicato M, Diederich M. Anti-inflammatory, pro-apoptotic, and anti-proliferative effects of a methanolic neem (azadirachta indica) leaf extract are mediated via modulation of the nuclear factor-kappaB pathway. *Genes Nutr* 2011;**6**:149–60
18. Thoh M, Kumar P, Nagarajaram HA, Manna SK. Azadirachtin interacts with the tumor necrosis factor (TNF) binding domain of its receptors and inhibits TNF-induced biological responses. *J Biol Chem* 2010;**285**:5888–95
19. Mattson MP, Camandola S. NF-kappaB in neuronal plasticity and neurodegenerative disorders. *J Clin Invest* 2001;**107**:247–54
20. Kawasaki T, Kawai T. Toll-like receptor signaling pathways. *Front Immunol* 2014;**5**:461
21. Duman EN, Kesim M, Kadioglu M, Yaris E, Kalyoncu NI, Erciyes N. Possible involvement of opioidergic and serotonergic mechanisms in antinociceptive effect of paroxetine in acute pain. *J Pharmacol Sci* 2004;**94**:161–5
22. Smith HS. Potential analgesic mechanisms of acetaminophen. *Pain Physician* 2009;**12**:269–80
23. Soares DG, Godin AM, Menezes RR, Nogueira RD, Brito AM, Melo IS, Coura GM, Souza DG, Amaral FA, Paulino TP, Coelho MM, Machado

RR. Anti-inflammatory and antinociceptive activities of azadirachtin in mice. *Planta Med* 2014;**80**:630–6
24. Pang Y, Lineaweaver WC, Lei MP, Oswald T, Shamburger S, Cai Z, Zhang F. Evaluation of the mechanism of vascular endothelial growth factor improvement of ischemic flap survival in rats. *Plast Reconstr Surg* 2003;**112**:556–64
25. Zhang F, Lineaweaver W. Acute and sustained effects of vascular endothelial growth factor on survival of flaps and skin grafts. *Ann Plast Surg* 2011;**66**:581–2
26. Wang Y, Chen SY, Gao WY, Ding J, Shi W, Feng XL, Tao XY, Wang L, Ling DS. Experimental study of survival of pedicled perforator flap with flow-through and flow-end blood supply. *Br J Surg* 2015;**102**:375–81
27. Ralay Ranaivo H, Hodge JN, Choi N, Wainwright MS. Albumin induces upregulation of matrix metalloproteinase-9 in astrocytes via MAPK and reactive oxygen species-dependent pathways. *J Neuroinammation* 2012;**9**:68
28. Lan L, Nakajima S, Wei L, Sun L, Hsieh CL, Sobol RW, Bruchez M, Van Houten B, Yasui A, Levine AS. Novel method for site-specific induction of oxidative DNA damage reveals differences in recruitment of repair proteins to heterochromatin and euchromatin. *Nucleic Acids Res* 2014;**42**:2330–45
29. Batinic-Haberle I, Tovmasyan A, Roberts ER, Vujaskovic Z, Leong KW, Spasojevic I. SOD therapeutics: latest insights into their structure-activity relationships and impact on the cellular redox-based signaling pathways. *Antioxid Redox Signal* 2014;**20**:2372–415
30. Terrazzano G, Rubino V, Damiano S, Sasso A, Petrozziello T, Ucci V, Palatucci AT, Giovazzino A, Santillo M, De Felice B, Garbi C, Mondola P, Ruggiero G. T cell activation induces CuZn superoxide dismutase (SOD)-1 intracellular re-localization, production and secretion. *Biochim Biophys Acta* 2014;**1843**:265–74
31. Boeke SJ, Boersma MG, Alink GM, van Loon JJ, van Huis A, Dicke M, Rietjens IM. Safety evaluation of neem (azadirachta indica) derived pesticides. *J Ethnopharmacol* 2004;**94**:25–41
32. Subapriya R, Nagini S. Medicinal properties of neem leaves: a review. *Curr Med Chem Anticancer Agents* 2005;**5**:149–6
33. Raizada RB, Srivastava MK, Kaushal RA, Singh RP. Azadirachtin, a neem biopesticide: subchronic toxicity assessment in rats. *Food Chem Toxicol* 2001;**39**:477–83

(Received April 27, 2020, Accepted July 31, 2020)